http://dx.doi.org/10.5012/bkcs.2012.33.3.1020

Comparison of Alternate Approaches for Reversible Geminate Recombination†

Svetlana S. Khokhlova and Noam Agmon*

The Fritz Haber Research Center, Institute of Chemistry, The Hebrew University of Jerusalem, Jerusalem 91904, Israel
**E-mail: agmon@fh.huji.ac.il*
Received December 7, 2011, Accepted January 20, 2012

This work compares various models for geminate reversible diffusion influenced reactions. The commonly utilized contact reactivity model (an extension of the Collins-Kimball radiation boundary condition) is augmented here by a volume reactivity model, which extends the celebrated Feynman-Kac equation for irreversible depletion within a reaction sphere. We obtain the exact analytic solution in Laplace space for an initially bound pair, which can dissociate, diffuse or undergo "sticky" recombination. We show that the same expression for the binding probability holds also for "mixed" reaction products. Two different derivations are pursued, yielding seemingly different expressions, which nevertheless coincide numerically. These binding probabilities and their Laplace transforms are compared graphically with those from the contact reactivity model and a previously suggested coarse grained approximation. Mathematically, all these Laplace transforms conform to a single generic equation, in which different reactionless Green's functions, $g(s)$, are incorporated. In most of parameter space the sensitivity to $g(s)$ is not large, so that the binding probabilities for the volume and contact reactivity models are rather similar.

Key Words : Diffusion, Feynman-Kac equation, Geminate reaction, Reversibility

Introduction

The study of diffusion influenced reactions is quite old,[1] and it builds upon even older results for the heat equation.[2] It has traditionally been limited to irreversible reactions.[3] The simplest case is that of geminate recombination namely, two particles (A and B) whose separation r changes by diffusion (in three dimensional space), and they may additionally undergo an association reaction

$$\mathrm{A} + \mathrm{B} \xrightarrow{k_a} \mathrm{C}. \tag{1.1}$$

When the motion of the particles is uncorrelated, their relative diffusion coefficient is $D = D_A + D_B$, the sum of their individual diffusion coefficients, D_A and D_B.

The reaction occurring at "contact" (i.e., at a specified distance of closest approach, σ, irrespective of the approach angle) was depicted by a boundary condition (BC) borrowed form the literature of the heat equation.[2] Smoluchowski assumed that every collision between A and B leads to reaction,[1] and this was described by an "absorbing" BC. Collins & Kimball[4] have considered the case that not every collision leads to reaction namely, the association rate coefficient k_a is finite. To depict this situation they have applied the "radiation" BC at $r = \sigma$. (This terminology arises because for the heat equation it describes heat loss from a solid's surface by radiation).[2] Subsequently, Wilemski & Fixman suggested that a more general formalism could use a "sink term" rather than a BC.[5] A delta-function sink-term at contact is equivalent to the radiation BC, but can be used also when a reaction occurs away from contact. In the absence of an interaction potential between A and B, the Collins-Kimball problem can be solved analytically.[3,4]

However, all chemical reactions are reversible to a certain extent, so that further generalization was required. A mathematical model for a geminate reversible diffusion influenced reaction

$$\mathrm{A} + \mathrm{B} \underset{k_d}{\overset{k_a}{\rightleftharpoons}} \mathrm{C}, \tag{1.2}$$

in which k_d is a dissociation rate coefficient (Fig. 1), was based on an extension of the Collins-Kimball formalism.[6,7] In the absence of an interaction potential, this contact reactivity model could be solved analytically (see below). The solution was first obtained for the initially bound pair,[8,9] and subsequently Kim & Shin[10] extended it to any initial separation. This solution has been further extended to the case that the reaction occurs in the excited-state, with different excited-state lifetimes for reactants and products.[11]

The contact reactivity model has been applied to data from experiment and simulation. Its numerical solution for Coulombic interaction between A and B has been applied to

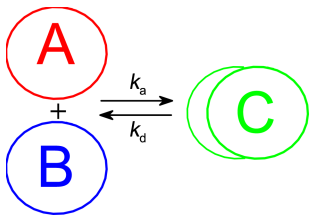

Figure 1. Schematic depiction of a reversible geminate reaction considered in this work.

†This paper is to commemorate Professor Kook Joe Shin's honourable retirement.

experimental data of excited-state proton transfer to solvent.[12,13] Its analytic solution in the absence of an interaction potential has been applied to liquid phase molecular simulations of hydrogen-bonded water molecule pairs,[14] and to protons in water.[15] In all these cases the observable was the binding probability for the initially bound state, C, denoted here by $Q(t)$. This function is thus also the focus of the present work.

However, there is an alternative description of irreversible geminate reactions, where association may occur uniformly within the volume V of the σ-sphere, with the rate coefficient k_a. The corresponding equation is well-known in the mathematical theory of diffusion,[16] because it is the Laplace transform (LT) of the residence (or occupation) time distribution,[17] and is often called the Feynman-Kac (FK) equation.[18,19] An analytic solution can be obtained only for its LT, which has to be inverted numerically into the time domain.

One may now generalize the FK equation by adding a dissociation term. This gives rise to two cases, depending on the nature of the dissociation process. (a) In the "sticky" case, C dissociates to give A and B separated to the same distance at which C was formed. (b) In the "mixed" case, C dissociates to give A and B separated uniformly within the reaction sphere.

To our knowledge, only case (b) was treated theoretically before in the context of the hydrogen-bond correlation function in liquid water.[20,21] The LT solution was presented without a detailed derivation. We provide the missing details that clarify the underlying assumptions in this approximation. However, an approximation is not really required for that problem, which can be solved exactly. In the present work we obtain the exact LT solution for $Q(t)$ for both cases of the volume reactivity model. Although the spatial density profiles differ between these cases, $Q(t)$ is identical. Moreover, we show that it obeys the same generic equation as in the contact reactivity model, only with a different "reactionless" Green's function.

This paper is structured as follows. We begin by proposing that both contact and volume reactivity models could be considered as special cases of a more general equation for "immobilization kinetics". We proceed by summarizing the expressions for the binding probability of the reversible Collins-Kimball equation ("contact reactivity"),[8-10] and then derive the exact LT solution for the two cases of the reversible Feynman-Kac equation ("volume reactivity"). The final Results section compares the various cases graphically, both in Laplace space and in the time domain.

Immobilization Kinetics

We begin with the myth of the Γοργωνν sisters: any human within their gaze would turn to stone. Our Gorgon sisters, A and B, may both freeze if they are within distance σ of one another. But later they may unfreeze and continue moving (randomly, of course, with a relative diffusion coefficient D). Their probability density (to be at distance r by time t) in their mobile state is denoted by $p(r,t)$, whereas $q(r,t)$ is the probability density in their frozen state. The freezing, or immobilization, probability per unit time within their "gazing sphere", $r \le \sigma$, is depicted by the rate function $k(r)$. Thus we assume that $k(r) \equiv 0$ for $r > \sigma$. The defrosting rate coefficient, k_d, is independent of position. In addition, there is an excluded volume interaction for a sphere of radius $\sigma_0 \le \sigma$, disallowing $r < \sigma_0$.

This immobilization process is described by two coupled partial differential equations:

$$\frac{\partial p(r,t)}{\partial t} = \mathcal{L}p(r,t) - k(r)p(r,t) + k_d q(r,t)\,, \tag{2.1a}$$

$$\frac{\partial q(r,t)}{\partial t} = k(r)p(r,t) - k_d q(r,t)\,, \tag{2.1b}$$

where $\mathcal{L}$ is the spherically symmetric diffusion operator in three dimensions,

$$\mathcal{L} = D\frac{1}{r^2}\frac{\partial}{\partial r}r^2\frac{\partial}{\partial r}\,. \tag{2.2}$$

Equation (2.1a) is supplemented by BCs when r tends to σ_0 or ∞:

$$r^2\partial p(r,t)/\partial r \to 0\,,\ r \to \sigma_0\,, \tag{2.3a}$$

$$p(r,t) \to 0\,,\ r \to \infty\,. \tag{2.3b}$$

Thus there is no flux into the excluded sphere, and no density at infinity. BCs are not required for Eq. (2.1b), in which r is just a parameter.

Here we consider only the initially immobilized state, so that $p(r,0)=0$. Additionally, in our model binding occurs only inside the sphere, hence $q(r,0) \equiv 0$ for $r \ge \sigma$. Because also $k(r) \equiv 0$ outside the σ-sphere, there is never any immobilized population with $r > \sigma$. We wish to calculate the immobilization probability at time t, which is defined by

$$Q(t) \equiv \int_{\sigma_0}^{\sigma} q(r,t)d^3r = 1 - \int_{\sigma_0}^{\infty} p(r,t)d^3r\,, \tag{2.4}$$

where $d^3r \equiv 4\pi r^2 dr$. Note that in the present exposition densities (with units of $1/r^3$) are denoted with lower-case symbols, whereas probabilities (that are dimensionless) are in upper-case.

The system of equations (2.1) can (in favorable cases) be solved by the LT technique, where the LT of a function $f(t)$ is defined as $\hat{f}(s) = \int_0^\infty e^{-st}f(t)dt$. This gives

Table 1. The terms $k(r)$ and $q(r,t)$ in Eq. (2.1), and the hard core distance σ_0 of Eq. (2.3a), for the contact reactivity model as compared with the two volume reactivity models treated in this work. D' is defined in Eq. (5.3b) below.

Model	$k(r)$	$q(r,t)$	σ_0
Contact reactivity	$k_a\frac{\delta(r-\sigma)}{4\pi\sigma^2}$	$\frac{\delta(r-\sigma)}{4\pi\sigma^2}Q(t)$	$\to\sigma$
Volume reactivity, $D'=0$	$\frac{k_a H(\sigma-r)}{V}$	$q(r,t)$	0
Volume reactivity, $D'=\infty$	$\frac{k_a H(\sigma-r)}{V}$	$\frac{H(\sigma-r)}{V}Q(t)$	0

$$s\hat{p}(r,s)-p(r,0)=\mathcal{L}\hat{p}(r,s)-k(r)\hat{p}(r,s)+k_d\hat{q}(r,s)\,, \qquad (2.5a)$$

$$\hat{q}(r,s)=\frac{1}{s+k_d}[k(r)\hat{p}(r,s)+q(r,0)]\,. \qquad (2.5b)$$

Utilizing the initial condition, $p(r,0)=0$, and inserting one equation into the other, we obtain an ordinary inhomogeneous differential equation for the LT of $p(r,t)$, namely

$$\{(s+k_d)\mathcal{L}-s[s+k_d+k(r)]\}\hat{p}(r,s)=-k_d q(r,0)\,, \qquad (2.6)$$

which we need to solve for the various cases under consideration.

The equations above are common to both contact and volume reactivity models considered below. In each of these cases $k(r)$, $q(r,t)$ and σ_0 may assume different values as summarized in Tbl. 1. Thus, in the familiar case that the reversible reaction occurs at contact,[8-10] σ_0 coincides with the contact distance σ and $k(r)$ is a delta-function sink there. In the volume reactivity models, when the reversible reaction occurs throughout the volume of the reaction sphere, $\sigma_0=0$ and $k(r)$ is a step-function sink in this volume. These models can have various variants depending on the fate of the immobilized state. When all immobilized population collects in a single bound state, $q(r,t)$ may be depicted as a normalized Heaviside function with amplitude $Q(t)$. A central goal of the present work is to calculate $Q(t)$ for the various models.

Contact Reactivity

The contact reactivity model of reversible geminate recombination[7-11] is a natural extension of the Collins-Kimball radiation boundary condition at contact. In this case $\sigma_0=\sigma$ namely, the particles do not penetrate into the reaction sphere. Rather, they react at its surface. This is where they get "immobilized". Hence we write this as a special case of the immobilization problem, where the immobilization rate function and the immobilized probability density are delta functions on the sphere's surface:

$$\frac{k(r)}{k_a}=\frac{\delta(r-\sigma)}{4\pi\sigma^2}=\frac{q(r,t)}{Q(t)}\,. \qquad (3.1)$$

Thus there is a single (r independent) bound state with probability $Q(t)$. It obeys an ordinary kinetic equation, $dQ(t)/dt=k_d p(\sigma,t)-k_d Q(t)$, which is obtained by inserting Eq. (3.1) into (2.1b) and integrating over space. With the initial condition $Q(0)=1$, its LT becomes:

$$(s+k_d)\hat{Q}(s)=1+k_a\hat{p}(\sigma,s)\,. \qquad (3.2)$$

We now rewrite the LT of $p(r,t)$, Eq. (2.6), as

$$(s+k_d)(\mathcal{L}-s)\hat{p}(r,s)=[sk_a\hat{p}(r,s)-k_d]\frac{\delta(r-\sigma)}{4\pi\sigma^2}\,. \qquad (3.3)$$

Because of the delta-function, one could equivalently replace $\hat{p}(r,s)$ on the right hand side (rhs) by $\hat{p}(\sigma,s)$, compare Eq. (2.15) in Ref. 22. In preparation for solving the volume reactivity problem below, we first reiterate the procedure for solving Eq. (3.3).

Solution in Laplace Space. In solving the differential equation (3.3), we note that on the left hand side (lhs) we have a LT of the diffusion equation in the absence of reaction, whereas the delta function on the rhs is its initial condition for pairs starting from $r=\sigma$. Denoting by $g(r,s|\sigma)$ the LT solution for reactionless diffusion ($k_a=k_d\equiv 0$) outside a reflecting sphere (for particles starting on its surface),

$$(\mathcal{L}-s)g(r,s|\sigma)=-\frac{\delta(r-\sigma)}{4\pi\sigma^2}\,, \qquad (3.4)$$

we try substituting $\hat{p}(r,s)=f(s)g(r,s|\sigma)$, where $f(s)$ is a function of s to be determined. The delta function now appears on both sides of Eq. (3.3). We do not divide by it, because it is identically zero almost everywhere. Instead, we integrate both sides, obtaining $f(s)=k_d/[s+k_d+sk_a g(\sigma,s|\sigma)]$. Inserting this into Eq. (3.2) gives

$$\hat{Q}(s)=\frac{1+k_a g(\sigma,s|\sigma)}{s+k_d+sk_a g(\sigma,s|\sigma)}\,, \qquad (3.5)$$

in full agreement with previous derivations.[8-11] This is actually a generic equation that holds for all the cases considered herein, only with different functions replacing $g(\sigma,s|\sigma)$.

Now the Green's function for free diffusion outside a reflecting sphere is, of course, well known.[2,3] At $r=\sigma$ it becomes:

$$g(\sigma,s|\sigma)^{-1}=k_D(1+\alpha\sigma)\,, \qquad (3.6)$$

where we have defined the diffusion-control rate coefficient by

$$k_D\equiv 4\pi\sigma D\,, \qquad (3.7)$$

and a scaled square-root of the Laplace variable by

$$\alpha\equiv\sqrt{s/D}\,. \qquad (3.8)$$

Time Domain. One can Laplace invert Eq. (3.5) analytically.[8-10] After inserting Eq. (3.6), the denominator of $\hat{Q}(s)$ becomes a cubic polynomial in α. Its three roots, $-x_1$, $-x_2$ and $-x_3$, obey the following system of algebraic equations:

$$x_1+x_2+x_3=-(1+k_a/k_D)/\sigma, \qquad (3.9a)$$

$$x_1x_2+x_2x_3+x_3x_1=k_d/D, \qquad (3.9b)$$

$$x_1x_2x_3=-k_d/(D\sigma). \qquad (3.9c)$$

These roots allow partial fraction decomposition of the polynomial into three terms, each being Laplace invertible. This finally gives

$$Q(t)=\sum_{i=1}^{3}\frac{-x_i(x_j+x_k)}{(x_j-x_i)(x_k-x_i)}\,\Omega(-x_i\sqrt{Dt})\,, \qquad (3.10)$$

where $i\neq j\neq k$. Here $\Omega(z)=\exp(z^2)\mathrm{erfc}(z)$, and $\mathrm{erfc}(z)$ is the complementary error function of a complex variable z.

Asymptotic Behavior. In the limit of short ($s\to\infty$) and long ($s\to 0$) times, Eq. (3.5) expands as

$$\hat{Q}(s)\sim\frac{1}{s+k_d}\,, \quad s\to\infty, \qquad (3.11a)$$

$$\hat{Q}(s) \sim \frac{1}{k_d} + \frac{K_{eq}}{k_D}(1-\alpha\sigma), \quad s \to 0 \tag{3.11b}$$

where

$$K_{eq} = k_a/k_d \tag{3.12}$$

is the equilibrium constant of reaction (1.2) in the association direction. These LTs are easily inverted into the time domain:

$$Q(t) \sim \exp(-k_d t), \quad t \to 0, \tag{3.13a}$$

$$Q(t) \sim \frac{K_{eq}}{(4\pi Dt)^{3/2}}, \quad t \to \infty. \tag{3.13b}$$

Asymptotic expansions are useful in comparing the different models discussed herein.

Volume Reactivity

The volume reactivity model of reversible geminate recombination is a natural extension of the FK equation, involving uniform reactivity within the σ-sphere. This means that $\sigma_0 \equiv 0$ namely, the particles can diffuse also within the reaction sphere, in which they react with a uniform rate coefficient, $k(r) = k_a/V \equiv k_r$. Starting from an initial bound state, $q(r,0)$, which is uniformly distributed within the reaction sphere, we may write the volume reactivity model as a special case of the immobilization problem,

$$\frac{k(r)}{k_a} = \frac{H(\sigma-r)}{V} = q(r,0). \tag{4.1}$$

Because bound A-B pairs are immobilized at their reaction distance, we term this the "sticky" volume reactivity model. In the present work, $H(x)$ denotes a Heaviside function, which is unity for $x \geq 0$ and zero otherwise, and the sphere's volume is

$$V = \frac{4}{3}\pi\sigma^3 = \int_0^\sigma H(\sigma-r)d^3r. \tag{4.2}$$

We also denote $k_a = Vk_r$. The factor V in Eq. (4.1) thus ensures that the initial distribution is normalized, $\int_0^\sigma q(r,0)d^3r \equiv Q(0) = 1$, and that the uniform recombination rate coefficient inside the sphere is k_r.

We now obtain from Eq. (2.6) that

$$(s+k_d)(\mathcal{L}-s)\hat{p}(r,s) = [sk_r\,\hat{p}(r,s) - k_d/V]\,H(\sigma-r). \tag{4.3}$$

This is the same as Eq. (3.3), only with $\delta(r-\sigma)/(4\pi\sigma^2)$ replaced by $H(\sigma-r)/V$. After solving Eq. (4.3) for $\hat{p}(r,s)$ one can obtain the LT of the binding probability from

$$(s+k_d)\,\hat{Q}(s) = 1 + k_r\hat{P}(\mathrm{B}_3,s), \tag{4.4}$$

which is obtained by inserting Eq. (4.1) into (2.5b) and integrating over space. Here B_3 denotes a three dimensional sphere of radius σ, and $\hat{P}(\mathrm{B}_3,s) \equiv \int_0^\sigma \hat{p}(r,s)d^3r$ is the LT of the residence probability within B_3. Thus Eq. (4.4) has the volume integral of the density instead of its surface value as in Eq. (3.2).

The solution can now be obtained in two different ways. The first is short and follows closely the derivation in the previous section. The second is longer, utilizing the standard route for solving inhomogeneous differential equations. Amusingly, the two routes produce expressions that appear different, yet they are numerically identical.

Fast Route. For contact reactivity we have utilized the Green's function, $g(r,s|\sigma)$, for the case of no reaction starting on the surface of a reflecting sphere. Here we consider the reactionless solution for an initially uniform distribution within B_3, which we denote by $g(r,s|\mathrm{B}_3)$:

$$(\mathcal{L}-s)g(r,s|\mathrm{B}_3) = -\frac{H(\sigma-r)}{V}. \tag{4.5}$$

As before, we assume a solution of the form

$$\hat{p}(r,s) = f(s)g(r,s|\mathrm{B}_3). \tag{4.6}$$

Substituting this into Eq. (4.3) and integrating over r gives, analogously, $f(s) = k_d/[s+k_d+sk_rG(\mathrm{B}_3,s|\mathrm{B}_3)]$, where for any initial condition $G(\mathrm{B}_3,s) \equiv \int_0^\sigma g(r,s)d^3r \equiv Vg(\mathrm{B}_3,s)$. Substituting into Eq. (4.4) gives the desired solution:

$$\hat{Q}(s) = \frac{1+k_a g(\mathrm{B}_3,s|\mathrm{B}_3)}{s+k_d+sk_a\,g(\mathrm{B}_3,s|\mathrm{B}_3)}. \tag{4.7}$$

This is completely analogous to the solution for surface reactivity in Eq. (3.5), with B_3 replacing σ. For free diffusion, the residence probability within a three dimensional sphere (for particles initially randomly distributed within this sphere) is known [e.g., Eq. (40) in Ref. 23]:

$$sG(\mathrm{B}_3,s|\mathrm{B}_3) = 1 - \frac{3(1+\alpha\sigma)}{(\alpha\sigma)^3}[\alpha\sigma\cosh(\alpha\sigma) - \sinh(\alpha\sigma)]e^{-\alpha\sigma}. \tag{4.8}$$

Note that $\hat{Q}(s) \approx G(\mathrm{B}_3,s|\mathrm{B}_3)$ when $k_r = k_d \to \infty$, provided that $sG(\mathrm{B}_3, s|\mathrm{B}_3) << 1$. The last two equations are the central results of this paper.

Standard Route. The standard route for solving Eq. (4.3) is to note that it is a second order linear inhomogeneous differential equation, with a special solution given by

$$\hat{p}(r,s) = \frac{k_d H(\sigma-r)/V}{s[s+k_d+k_r H(\sigma-r)]}. \tag{4.9}$$

To this, one should add a linear combination of the two solutions of the homogeneous equation, with the two coefficients determined from the boundary conditions for $r \to 0$ and $r \to \infty$ in Eq. (2.3). Define a new independent variable, y, by

$$y = \left(1 + \frac{k_r H(\sigma-r)}{s+k_d}\right)^{1/2} \alpha r. \tag{4.10}$$

The homogeneous equation can then be rewritten as

$$\left(\frac{1}{y^2}\frac{\partial}{\partial y}y^2\frac{\partial}{\partial y} - 1\right)\hat{p}(y) = 0. \tag{4.11}$$

The two linearly independent solutions of this equation are $\exp(\pm y)/y$. Inside the sphere $\hat{p}(y) = \sinh(y)/y$ is the required linear combination, because it obeys $y^2 d(\sinh(y)/y)/dy \to 0$ as $y \to 0$. Outside the ball the solution is $\exp(-y)/y$, because

it decays to 0 as $y \to \infty$. Therefore the solution inside and outside the sphere becomes:

$$\hat{p}(r,s)=\frac{k_d/V}{s(s+k_d+k_r)}+\frac{A}{r}\sinh(\beta r), \quad r\le\sigma, \tag{4.12a}$$

$$\hat{p}(r,s)=\frac{B}{r}e^{-\alpha r}, \quad r\ge\sigma, \tag{4.12b}$$

where α is defined in Eq. (3.8), whereas β is defined by

$$\beta=\left(1+\frac{k_r}{s+k_d}\right)^{1/2}\alpha. \tag{4.13}$$

The coefficients A and B are finally obtained from the continuity of the solution and its first derivative at $r=\sigma$, giving:

$$\hat{p}(r,s)=\frac{k_d/V}{s(s+k_d+k_r)}\left[1-\frac{(1+\alpha\sigma)\sinh(\beta r)}{\beta r\cosh(\beta\sigma)+\alpha r\sinh(\beta\sigma)}\right], \; r\le\sigma, \tag{4.14a}$$

$$\hat{p}(r,s)=\frac{k_d/V}{s(s+k_d+k_r)}\frac{\beta\sigma\coth(\beta\sigma)-1}{\beta r\coth(\beta\sigma)+\alpha r}e^{-\alpha(r-\sigma)}, \; r\ge\sigma. \tag{4.14b}$$

Inserting Eq. (4.14a) into (2.5b) finally gives

$$(s+k_d)V\hat{q}(r,s)=1+\frac{k_rk_d}{s(s+k_d+k_r)}\left[1-\frac{(1+\alpha\sigma)\sinh(\beta r)}{\beta r\cosh(\beta\sigma)+\alpha r\sinh(\beta\sigma)}\right], \tag{4.15}$$

so that after integration over the volume of the ball we get

$$(s+k_d)\hat{Q}(s)=1+\frac{k_rk_d}{s(s+k_d+k_r)}\left[1-\frac{3(1+\alpha\sigma)}{(\beta\sigma)^2}\frac{\beta\sigma\coth(\beta\sigma)-1}{\beta\sigma\coth(\beta\sigma)+\alpha\sigma}\right]. \tag{4.16}$$

This result appears to be quite different from Eq. (4.7), but in fact the two coincide within numerical accuracy. This suggests that the two expressions are identical, both being exact solutions of the same equation, yet it is difficult to show this directly.

Asymptotic Behavior. The limits of short and long times of the binding probability are obtained from the limits of large and small s, respectively, in either Eq. (4.7) or (4.16). At large s, it is immediately evident from Eq. (4.16) that

$$\hat{Q}(s)\sim\frac{1}{s+k_d}, \quad s\to\infty, \tag{4.17}$$

so that, as for the contact reactivity model, the initial decay is exponential, $\exp(-k_dt)$.

The small s behavior is a bit more involved. We start from the corresponding behavior of the residence probability, $G(B_3,s|B_3)$ in Eq. (4.8). The exponential terms there need be expanded to fourth order. Alternately, one may integrate $g(r,s|B_3)$, Eq. (49) of Ref. 19, over B_3. Dividing by V, we obtain

$$g(B_3,s|B_3)\sim\frac{1}{k_D}\left(\frac{6}{5}-\alpha\sigma\right), \quad s\to 0. \tag{4.18}$$

Now we neglect the terms proportional to s in the denominator of Eq. (4.7), so that $\hat{Q}(s)\sim[1+k_ag(B_3,s|B_3)]/k_d$. Subsequently, we obtain that

$$\hat{Q}(s)\sim\frac{1}{k_d}+\frac{K_{eq}}{k_D}\left(\frac{6}{5}-\alpha\sigma\right), \quad s\to 0. \tag{4.19}$$

This differs from the contact reactivity asymptotics in Eq. (3.11b) by the factor 6/5 replacing 1 there. The time domain asymptotics is thus identical, see Eq. (3.13b).

Single Bound State

Exact Solution. The sticky volume reactivity model discussed above has many bound states, because the pair can become immobilized at any $0\le r\le\sigma$. It may be interesting to consider also the case of a single bound state, in which products are collected from the whole reaction sphere.

Therefore instead of Eq. (4.1) we assume

$$\frac{k(r)}{k_a}=\frac{H(\sigma-r)}{V}=\frac{q(r,t)}{Q(t)}. \tag{5.1}$$

Evidently, $Q(t)$ is still the spatial integral of $q(r,t)$, which is now restricted to be a step function. This differs from $q(r,t)$ of Eq. (4.15), which does vary with r within the reaction sphere. Nevertheless, we argue that $Q(t)$, the overall binding probability, is exactly the same, and is thus given by Eq. (4.7). This follows because, for $Q(0)=1$, Eq. (5.1) at $t=0$ reduces to Eq. (4.1), so that all subsequent equations leading to Eq. (4.7) remain unchanged.

In the present mixed case the time dependence of $Q(t)$ follows a simple kinetic equation

$$dQ(t)/dt=k_rP(B_3,t)-k_dQ(t), \tag{5.2}$$

obtained by inserting Eq. (5.1) into Eq. (2.1b) and integrating over space. As before, $P(B_3,t)\equiv\int_0^\sigma p(r,t)d^3r$.

One can obtain the two volume reactivity models as two limiting cases of a generalized equation for $dQ(t)/dt$, with added diffusion of the bound pairs within B_3. Thus we replace Eq. (2.1) by

$$\frac{\partial p(r,t)}{\partial t}=\mathcal{L}p(r,t)-k_rH(\sigma-r)p(r,t)+k_dq(r,t), \tag{5.3a}$$

$$\frac{\partial q(r,t)}{\partial t}=\mathcal{L}'q(r,t)+k_rH(\sigma-r)p(r,t)-k_dq(r,t). \tag{5.3b}$$

Here $\mathcal{L}'$ is a diffusion operator, as in Eq. (2.2), only with a distance dependent diffusion coefficient

$$D(r)=D'H(\sigma-r), \tag{5.4}$$

which is also a step-function within B_3. When $D'=0$ we recover the previous "sticky" situation, Eq. (2.1b), of multiple bound states that do not interconvert. In the opposite limit ($D'\to\infty$) the bound state is "well stirred", or "mixed", and this erases any r dependence so that $q(r,t)$ becomes a step-function as in Eq. (5.1). This is useful because the coupled partial differential equations (5.3) can be easily solved numerically for any value of D', for example by the Windows application for solving the spherically symmetric diffusion

problem, SSDP (ver. 2.66).[24]

The Luzar-Chandler (LC) Approximation. We have seen that the coupled diffusion equations can be solved exactly for $\hat{Q}(s)$ in both limits of D', and this solution is given by Eqs. (4.7) and (4.8). Thus, in the continuum limit of random walks considered here, there is no need for any approximation. An alternative treatment, used in a paper on hydrogen bond dynamics,[20] employs instead a coarse grained approximation, obtaining similar results. We reproduce here the details of that approach[25] as they have not yet been provided in the literature. An analogous treatment may be useful for similar problems for which an exact solution is unavailable.

The derivation of the LC approximation is based on a further Fourier transform (FT) of the diffusion equations, where a FT of a function $f(x, y, z)$ in the Cartesian coordinates x, y and z, is

$$\tilde{f}(\omega_x,\omega_y,\omega_z)=\iiint_{-\infty}^{\infty} f(x,y,z)\exp[-\imath(\omega_x x+\omega_y y+\omega_z z)]dxdydz\,, \tag{5.5}$$

where $\imath\equiv\sqrt{-1}$. Thus the FT of the Laplacian is $\widetilde{\Delta f}=-\omega^2\tilde{f}$, where $\omega^2=\omega_x^2+\omega_y^2+\omega_z^2$, and the FT of a delta function is 1. Noting that the volume of the ball is small, the following two approximations are introduced

$$\tilde{H}(\sigma-r)\approx V\,, \tag{5.6a}$$

$$p(r,t)\approx p(0,t)\ \text{ for } r\le\sigma, \tag{5.6b}$$

where the first equation also approximates the sphere by a cube.

With these assumptions, one may FT Eq. (4.3) to obtain

$$(s+k_d)(s+\omega^2 D)\tilde{p}(\omega,s)=k_d-sk_a\hat{p}(0,s)\,. \tag{5.7}$$

The inverse FT is given by Eq. (5.5) with $\imath$ replaced by $-\imath$, and division by $(2\pi)^3$. Dividing Eq. (5.7) by $s + \omega^2 D$, taking its inverse FT and setting $r = 0$ gives

$$[s+k_d+sk_a g(s)]\hat{p}(0,s)\ =k_d g(s), \tag{5.8}$$

where $g(s)$ is defined by

$$g(s)=\frac{1}{(2\pi)^3}\int_0^{\omega_c}\frac{d^3\omega}{s+D\omega^2}\,, \tag{5.9}$$

the inverse FT of $(s + D\omega^2)^{-1}$ at the origin, which is now written in spherical coordinates.

The above integral diverges when the upper limit is infinite. This is due to the coarse-graining approximations introduced above. To compensate for this, oscillations with wavelengths smaller than σ have to be truncated at some cutoff angular frequency ω_c. In spherical symmetry, we demand that Eq. (5.9) gives the correct $s\to\infty$ limit of $Vg(s) \to 1/s$, which is immediate from Eq. (4.8). This implies that

$$\frac{V}{(2\pi)^3}\int_0^{\omega_c} d^3\omega=1\ \Rightarrow\ \omega_c=(9\pi/2)^{1/3}/\sigma. \tag{5.10}$$

This condition differs somewhat from the value of ω_c in Cartesian coordinates utilized in Refs. 20 and 21, and provides a better agreement with the exact result, which was obtained above for a reactive sphere (rather than a cube). Admittedly, this is still somewhat arbitrary. However, it does not affect the leading terms in either the short- or long-time asymptotic expansion (obtained below), which are exact. This may be one reason for the success of this approximation.

To evaluate the integral in Eq. (5.9) we rewrite $x^2/(1 + x^2)$ as $1-1/(1 + x^2)$. Performing the two definite integrals gives

$$g(s)=\frac{\omega_c}{2\pi^2 D}\left[1-\frac{\alpha}{\omega_c}\arctan\left(\frac{\omega_c}{\alpha}\right)\right]. \tag{5.11}$$

Finally, the binding probability is given by Eq. (4.4), so that

$$\hat{Q}(s)=\frac{1+k_a g(s)}{s+k_d+sk_a g(s)}\,. \tag{5.12}$$

This has identical form to Eqs. (3.5) and (4.7), only the function $g(s)$ differs.

We now show that the LC approximation has the correct asymptotics. The $s\to\infty$ limit is independent of $g(s)$, so that $\hat{Q}(s)\to 1/(s+k_d)$. It remains to consider the small s limit, which follows by neglecting the term $s[1 + k_a g(s)]$ in the denominator of Eq. (5.12) and setting $\arctan(\infty) = \pi/2$. This gives

$$\hat{Q}(s)\sim\frac{1}{k_d}+\frac{K_{eq}}{k_D}\left[\frac{2\omega_c\sigma}{\pi}-\alpha\sigma\right],\ s\to 0. \tag{5.13}$$

This result should be compared with Eqs. (3.11b) and (4.19).

With ω_c value from Eq. (5.10), the constant $2\omega_c\sigma/\pi = (6/\pi)^{2/3}$. However, it does not affect the long time behavior [as it gives a $\delta(t)$ term when inverted], which is determined from the $\sqrt{s}$ term. Hence the long-time asymptotics is the same as in Eq. (3.13b).

Results and Discussion

Contact reactivity models for reversible geminate reactions have been used for quite some time.[6-15] In a seminal work, Kim and Shin have provided the full solution for the probability density in this case.[10] Reversible volume reactivity models have attracted less attention, although in the irreversible case they correspond to the celebrated FK equation. Such a model has been solved approximately in the context of water dynamics.[20,21] However, systematic analytical treatment and comparison with the alternate approaches has not been attempted. In the present work we have focussed on two limiting cases of volume reactivity models, in which the reacting pair becomes immobilized at the distance where reaction occurs ($D' = 0$), or else the products are "mixed" within the reaction volume ($D' = \infty$) so that in effect there is a single bound state.

Figure 2 compares the probability densities of free and bound pairs, $p(r,t)$ and $q(r,t)$, for these two cases, as calculated from a numerical solution of Eqs. (5.3).[24] We set the distance and time scales such that $\sigma = 1$ and $D = 1$. Both cases begin from a uniformly distributed bound state, so that $p(r, 0) = 0$ whereas $q(r, 0)$ is a step-function. With time,

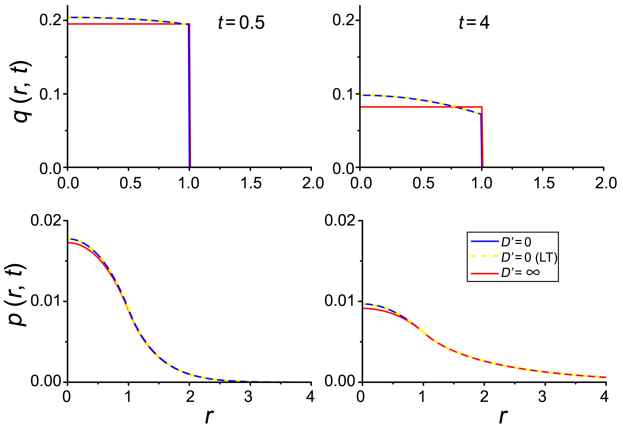

Figure 2. Time dependence of the density profiles for bound and unbound pairs, $q(r,t|B_3)$ (top rows) and $p(r,t|B_3)$ (bottom rows), for the two volume reactivity models with $D' = 0$ and ∞ in Eq. (5.3b), and at two different times (left *vs.* right columns). Calculated numerically using SSDP, ver. 2.66,[24] with two diffusion levels (for unbound and bound pairs). In the case that $D' = 0$, the densities were also calculated by Laplace inversion[26] of Eqs. (4.14) and (4.15), respectively (dashed yellow lines). The agreement verifies our analytic solutions. The parameters are: $\sigma = 1$ and $D = 1$ (setting the distance and time units), $k_d = 0.5$ and $k_a = k_D = 4\pi\sigma D \approx 12.57$.

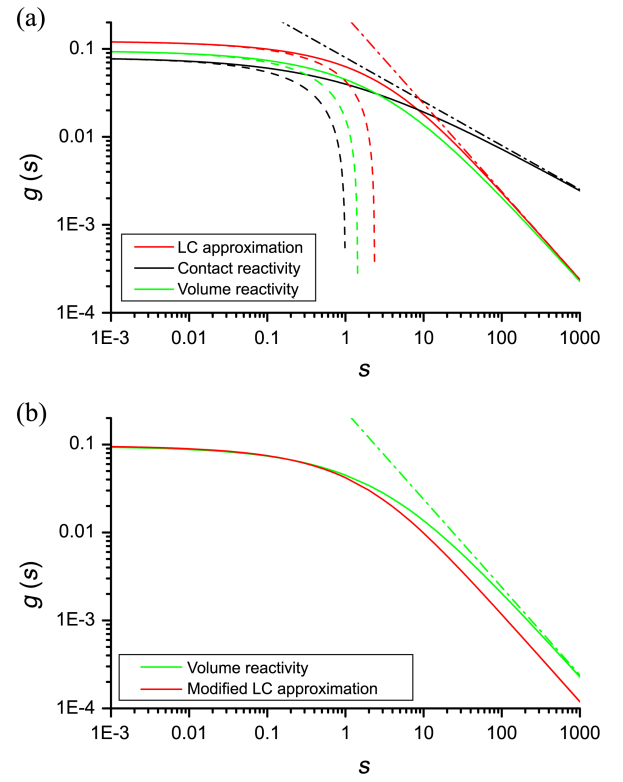

Figure 3. (a) The s dependence of the g-functions for the different models: Contact reactivity, Eq. (3.6); Volume reactivity, Eq. (4.8); LC approximation, Eq. (5.11). Dashed lines are its small s expansions: $k_D g(s) \sim 1 - \alpha\sigma$, $6/5 - \alpha\sigma$ and $2\omega_c\sigma/\pi - \alpha\sigma$, respectively. Dash-dot lines are its large s expansions: $g(s) \sim (k_D\alpha\sigma)^{-1}$ and $(Vs)^{-1}$. The parameters, σ, D, k_a and k_d, are as in Figure 2. (b) The modified LC g-function, obtained by setting the rhs of Eq. (5.10) to 1/2 instead of 1 [so that $\omega_c = (9\pi/4)^{1/3}/\sigma$], as compared with the volume reactivity model from panel (a).

dissociation creates unbound pairs with a distribution $p(r, t)$ that "spills-over" by diffusion beyond the sphere's radius, σ.

When $D' = \infty$, $q(r, t)$ indeed remains a step-function for all times. For $D' = 0$, it gradually becomes non-uniform, with the density at the rim depleting faster than in the center. Therefore, the two profiles intersect somewhere within the sphere, becoming more dissimilar with increasing time. Nevertheless, $r^2q(r, t)$ is much closer for the two cases, and, amusingly, their integrals precisely coincide. Thus there is just a single expression for $Q(t)$, whose LT is given by Eqs. (4.7) and (4.8). Note also that for $D' = 0$ we have obtained $\hat{q}(r,t)$ and $\hat{p}(r,t)$ in Eqs. (4.14) and (4.15), and their numerical Laplace inversion[26] coincides with the numerical solution of Eqs. (5.3).

$\hat{Q}(s)$ or $Q(t)$ do differ between the volume and contact reactivity models. However, they obey the same generic equation, only with a different function $g(s)$. For contact reactivity this is Eq. (3.5),[8-11] with $g(s) \equiv g(\sigma,s|\sigma)$ from Eq. (3.6). For volume reactivity this is Eq. (4.7), with $g(s) \equiv G(B_3,s|B_3)/V$ from Eq. (4.8). For the LC approximation this is Eq. (5.12) with $g(s)$ from Eq. (5.11). These three g-functions are compared in Figure 3. The contact and volume reactivity models differ quite considerably at large s, behaving asymptotically like $s^{-1/2}$ and s^{-1}, respectively. The g-function for the LC approximation is quite close to the exact result for volume reactivity. The choice of ω_c in Eq. (5.10) ensures that both have the same large-s behavior. Alternately, ω_c can be chosen so that their small-s behavior is approximately the same, giving the modified LC approximation in panel (b).

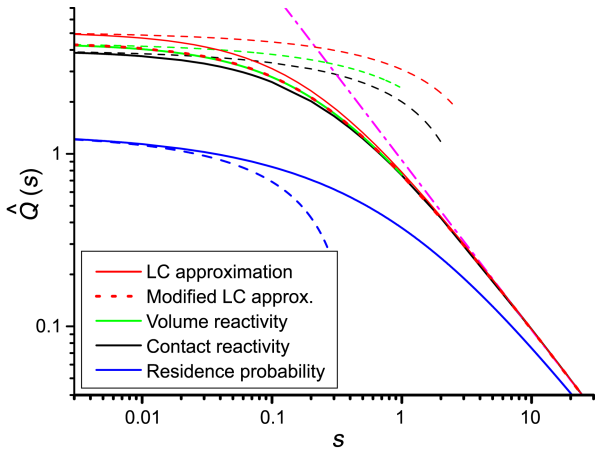

Figure 4. The s dependence of the LT of the binding probability for an initially bounded pair as calculated for the different models: Contact reactivity, Eqs. (3.5) and (3.6), black line; Volume reactivity, Eqs. (4.7) and (4.8), green line; LC approximation, Eqs. (5.11) and (5.12), red line. The modified LC approximation, obtained by setting the rhs of Eq. (5.10) to 1/2, is shown by the dotted red line. The parameters, σ, D, k_a and k_d, are as in Figure 2. Dashed lines of matching colors demonstrate the $s \to 0$ asymptotics, from Eqs. (3.11b), (4.19) and (5.13). Dash-dotted magenta line is $1/s$, the $s \to \infty$ limit. Blue line is the LT of the residence probability from Eq. (4.8), with $\sigma = R = 1.817$, corresponding to a sphere of volume $K_{eq} \equiv k_a/k_d = 25.13$. Dashed blue line is its small s expansion from Eq. (4.18).

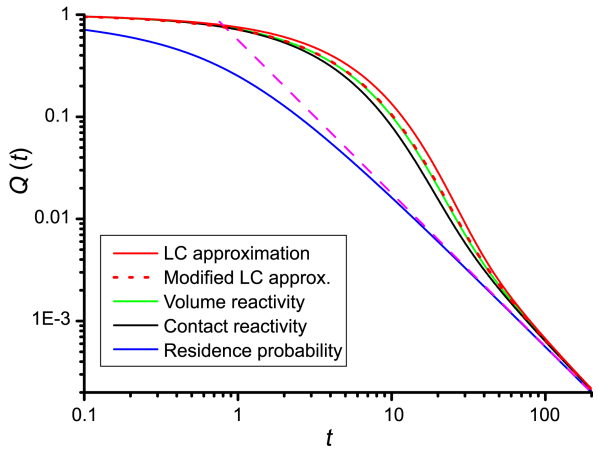

Figure 5. The binding probabilities as functions of time for the different reversible geminate models, obtained by numerical inversion[26] of the LTs depicted in Figure 4. For the contact reactivity model and the residence probability there are analytic results in the time domain: Eq. (3.10) here and Eq. (41) in Ref. 23, respectively. For volume reactivity we have also obtained $Q(t)$ by numerical integration[24] of Eq. (5.3) with $D' = 0$. These solutions are in perfect agreement with the inverted LTs. Dashed magenta line is the universal long-time behavior from Eq. (3.13b).

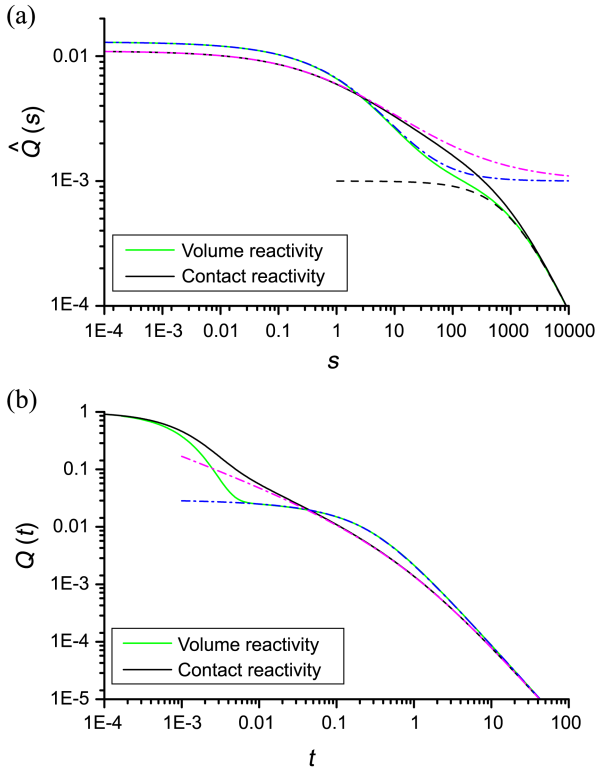

Figure 6. (a) Comparison of the LT of the binding probability for the contact and volume reactivity models, Eq. (3.5) and Eq. (4.16), reactivity. As before, $\sigma = 1$ and $D = 1$, whereas $k_a = 10k_D \approx 125.7$ and $k_d = 1000$. The dash-dotted blue and magenta lines correspond to the large k_d behavior, $k_d\hat{Q}(s) \sim 1 + k_a g(s)$, with the corresponding g-functions. The black dashed line represents the $s \to \infty$ behavior, $1/(s + k_d)$. (b) The numerically inverted binding probabilities, $Q(t)$, for the two reactivity models, with their long-time asymptotics.

The functions $\hat{Q}(s)$ and $Q(t)$ for the three g-functions are shown in Figures 4 and 5, respectively. In spite of the large difference between the g-functions for the contact and volume models at large s, the differences in the binding probabilities are rather small, because $g(s)$ becomes negligibly small in this limit. The large s behavior, $\hat{Q}(s) \sim (s + k_d)^{-1}$, is thus independent of $g(s)$. The $s^{1/2}$ term in the small s behavior coincides in all these cases, and inverts to give the ubiquitous $t^{-3/2}$ long-time asymptotics, Eq. (3.13b), which is depicted by the dashed magenta line in Figure 5. The LC approximation is close to the exact solution for volume reactivity, and the modified LC approximation is almost indistinguishable from it.

In comparison we show also the behavior of the residence probability from Eq. (4.8), which can be inverted analytically.[23] It could model an ultrafast reaction for which $k_r = k_d \to \infty$. Here the pair may be considered as "bound" simply if their separation is below some value R. At long times, it also exhibits a $t^{-3/2}$ behavior, only with the volume $4\pi R^3/3$ replacing K_{eq} in Eq. (3.13b).[23] Therefore, in this comparison we have chosen $R = (3K_{eq}/4\pi)^{1/3}$ so that the long time asymptotics coincide. (Note that $R = \sigma$ when $k_r = k_d$). Aside from that, the behavior of $G(B_3,t|B_3)$ differs from $Q(t)$, which contains explicit reaction terms. It approaches the $t^{-3/2}$ limiting behavior from below, whereas the rate-models approach it from above (Fig. 5), and its short time behavior follows a $t^{1/2}$ power-law rather than being exponential, $\exp(-k_d t)$, as for the rate models.

Finally, we have scanned the parameter space by keeping D and σ unity and varying k_a and k_d. We have found that the behavior seen in Figures 4 and 5, with little difference between the models, is rather typical. However, we have also found more complex behavior, when the contact and volume models differ at intermediate times, such as shown in Figure 6. In this case ($k_d >> k_r > k_D$) the binding probability decays in two phases: First there is dissociation, and only later diffusion and recombination come into play.

In conclusion, we have derived here exact results for the volume reactivity models of reversible geminate pairs, which start from their bound state. Two cases were considered, which differ in the definition of their bound state: "sticky" ($D' = 0$) *vs.* "mixed" ($D' = \infty$). Interestingly, only small differences exist between the pair distribution functions of these two models, while their binding probabilities, $Q(t)$, are exactly the same. Moreover, $Q(t)$ from the more widely utilized contact reactivity model is quite similar, and so is an approximate coarse grained solution.[20,21] Thus it appears that $Q(t)$ alone might not be a very sensitive indicator for selecting the most appropriate kinetic model, an observation previously made in a comparison of the contact reactivity model with water simulations.[14] The complete Green's function solution for various initial separations may better distinguish between the various models.

Acknowledgments. We thank Alenka Luzar for her handwritten notes and Attila Szabo for comments on the ms. Research supported by THE ISRAEL SCIENCE FOUND-

ATION (grant number 122/08). The Fritz Haber Center is supported by the Minerva Gesellschaft für die Forschung, München, FRG.

References

1. von Smoluchowski, M. Z. *Physik. Chem.* **1917**, *92*, 129-168.
2. Carslaw, H. S.; Jaeger, J. C. *Conduction of Heat in Solids*, 2nd ed.; Oxford University Press: Oxford, 1959.
3. Rice, S. A. *Diffusion-Limited Reactions*; Elsevier: Amsterdam, 1985; Vol. 25.
4. Collins, F. C.; Kimball, G. E. *J. Colloid Sci.* **1949**, *4*, 425-437.
5. Wilemski, G.; Fixman, M. *J. Chem. Phys.* **1973**, *58*, 4009-4019.
6. Goodrich, F. C. *J. Chem. Phys.* **1954**, *22*, 588-594.
7. Agmon, N. *J. Chem. Phys.* **1984**, *81*, 2811-2817.
8. Agmon, N.; Weiss, G. H. *J. Chem. Phys.* **1989**, *91*, 6937-6942.
9. Agmon, N.; Szabo, A. *J. Chem. Phys.* **1990**, *92*, 5270-5284.
10. Kim, H.; Shin, K. J. *Phys. Rev. Lett.* **1999**, *82*, 1578-1581.
11. Gopich, I. V.; Agmon, N. *J. Chem. Phys.* **1999**, *110*, 10433-10444.
12. Pines, E.; Huppert, D.; Agmon, N. *J. Chem. Phys.* **1988**, *88*, 5620-5630.
13. Agmon, N. *J. Phys. Chem. A* **2005**, *109*, 13-35.
14. Markovitch, O.; Agmon, N. *J. Chem. Phys*. **2008**, *129*, 084505.
15. Chen, H.; Voth, G. A.; Agmon, N. *J. Phys. Chem. B* **2010**, *114*, 333-339.
16. Karlin, S.; Taylor, H. M. *A Second Course in Stochastic Processes*; Academic Press: San-Diego, 1981.
17. Kac, M. On Some Connections between Probability Theory and Differential and Integral Equations. *Proc. 2nd Berkeley Symp. Mathematical Statistics and Probability*, Berkeley, 1951; pp 189-215.
18. Majumdar, S. N. *Curr. Sci.* **2005**, *89*, 2076-2092.
19. Agmon, N. *J. Phys. Chem. A* **2011**, *115*, 5838-5846.
20. Luzar, A.; Chandler, D. *Nature* **1996**, *379*, 55-57.
21. Luzar, A. *J. Chem. Phys.* **2000**, *113*, 10663-10675.
22. Gopich, I. V.; Solntsev, K. M.; Agmon, N. *J. Chem. Phys.* **1999**, *110*, 2164-2174.
23. Agmon, N. *Phys. Chem. Chem. Phys.* **2011**, *13*, 16548-16557.
24. Krissinel', E. B.; Agmon, N. *J. Comput. Chem.* **1996**, *17*, 1085-1098.
25. Luzar, A. Private communication.
26. Abate, J.; Whitt, W. *ORSA J. Comput.* **1995**, *7*, 36-43.